

“十二五”国家重点图书

Advances  
in  
Materials  
and  
Mechanics

# Advances in Cell Mechanics

细胞力学进展 (英文版)

Xibao Lixue Jinzhan

Edited by Shaofan Li and Bohua Sun

# Preface

During the past decade, molecular and cellular biophysics has emerged as one of the most active and exciting areas at the frontier of scientific research. It is a multi-disciplinary field that has many important applications in medicine, health care, life science and biology in general. In essence, the origins of many diseases and illness are rooted at the cellular level. Like molecular and cellular biology, molecular and cellular biophysics is also an indispensable part of the very foundation of contemporary medical and life sciences. In fact, cellular biophysics not only provides a theoretical foundation toward understanding biological processes such as the function of organs, tissues and their interactions, but also provides practical answers to medical treatment and pathology including molecular mechanism of diseases and infections. Because of rapid development of nano-science and nano-technologies, molecular and cellular biophysics not only offers a practical means but also the promise to treat and cure many diseases with which we as a human society are still struggling with. However, unlike molecular cellular biology, molecular and cellular biophysics, in particular molecular and cellular biomechanics, is still a field at its infancy. It is precisely because of this that makes cellular mechanics a promising and exciting research field to study and to work.

In this book, we have selected nine research works at the forefront of molecular and cellular biomechanics to be introduced to our readers. It is our opinion that these works represent the current trend and future directions of cellular biomechanics research. By compiling these different topics into one volume, a unique perspective is provided on the current state of cell mechanics research and what lies in the future.

Among these contributions, Romero and Arribas presented their groundbreaking work on three-dimensional cell model, cell growth dynamics algorithm, and associated large-scale finite element simulation through Chapter 1. In Chapter 2, Zeng, Li, and Kohles presented their work on multiscale simulations of soft contact and adhesion of stem cells. In this work, a soft matter model has been developed to model the mechanical mechanism of the mechanotransduction of stem cells. Focusing on molecular mechanics and genetic mechanism of cellular biology, Wu, Wang, and Cohen presented their molecular dynamics modeling of proteins in Chapter 3. More specifically, they employed a molecular dynamics and principal component analysis (MD-PCA) approach studying sickle hemoglobin-hemoglobin interaction, which is the main cause of sickle cell anemia. In Chapter 4, Qin, Chou, Kreplak, and Buehler presented their latest work on atomistic and coarse-grain modeling and simulations of cellular intermediate filaments. They not only presented their own work, but also provided a detailed tutorial on modeling and simulations of intermediate filament networks. Complementary to Qin et al's work, in Chapter 5, Hatami-Marbini and Mofrad give a tutorial overview of

cytoskeletal mechanics and rheology, and the topics that they have touched on are from mechanics of intermediate filament, rheology of cytoskeleton network, experimental measurements and techniques, to computation and simulation approach. To capture the complexity of cell's constitutive behaviors, in Chapter 6, Vernerey presented a multiphase mixture cell model and its application to cell-substrate interactions. In the proposed multiphase cell model, it combines the continuum description of the stress fiber, mass transport, cytosol fluid motion, and G-actin monomer motion, etc. Not only does the multiphysics model couple and combine several different aspects of cell biology, but the author has also applied the latest extended finite element method (X-FEM) and level-set method to simulate cell contact and adhesion with an extracellular substrate. This has demonstrated how applied and computational mechanics can solve complex problems in cell mechanics. To investigate mechanotransduction of cells through a purely thermodynamic approach, Sarvestani presented his analytical cell adhesion model in Chapter 7 that takes into account the effects of substrate stiffness and how it affects the growth of nascent adhesion areas. In Chapter 8, Kohles provided a detailed account on the experimental biomechanics of a single cell, in which he has discussed a state-of-the-art opto-hydrodynamics technique for measuring isolated cellular mechanical properties. Finally, in Chapter 9, Shen discussed his nonlocal shell model to simulate the buckling of microtubules inside a cell. This is a good example that clearly shows how non-classical continuum mechanics can contribute to the understanding of cellular biology.

Finally, it is our hope that this volume will disseminate much useful information in cellular biomechanics to a larger community outside the area of applied mechanics, while arousing public interest in cell mechanics research and applications. Ultimately, we envision that these works would promote more in-depth study and research in cell mechanics and cellular biophysics.

Shaofan Li and Bohua Sun  
February 4, 2011

2.3.2	The cohesive contact model . . . . .	36
2.4	Meshfree Galerkin formulation and the computational algorithm . . . . .	38
2.5	Numerical simulations . . . . .	40
2.5.1	Validation of the material models . . . . .	41
2.5.2	Cell response in four different stiffness substrates . . . . .	42
2.5.3	Cell response to a stiffness-varying substrate . . . . .	45
2.5.4	Comparison of two different contact algorithms . . . . .	47
2.5.5	Three-dimensional simulation of cell spreading . . . . .	47
2.6	Discussion and conclusions . . . . .	50
	References . . . . .	51

### **Chapter 3 Modeling of Proteins and Their Interactions with Solvent . . . . .**

		55
3.1	Introduction . . . . .	55
3.2	Classical molecular dynamics . . . . .	58
3.2.1	Coarse-grained model . . . . .	59
3.2.2	High performance computing . . . . .	62
3.3	Principal component analysis . . . . .	62
3.3.1	Three oscillators system analysis with PCA . . . . .	64
3.3.2	Quasi-harmonic analysis . . . . .	72
3.3.3	Equilibrium conformational analysis . . . . .	73
3.4	Methods and procedures . . . . .	74
3.4.1	Framework . . . . .	74
3.4.2	Overlap coefficients . . . . .	74
3.4.3	Correlation analysis . . . . .	75
3.4.4	PCA with MD simulation . . . . .	76
3.4.5	Kabsch algorithm . . . . .	79
3.4.6	Positional correlation matrix . . . . .	80
3.4.7	Cluster analysis . . . . .	80
3.5	MD simulation with T4 lysozyme . . . . .	81
3.5.1	Equilibration measures . . . . .	83
3.5.2	Fluctuation analysis . . . . .	84
3.5.3	Mode selection and evaluation . . . . .	85
3.5.4	Eigenvalue analysis . . . . .	86
3.5.5	Overlap evaluation . . . . .	89
3.5.6	Identification of slow conformational flexibility . . . . .	96
3.5.7	Correlation analysis of T4 lysozyme . . . . .	96
3.6	Hemoglobin and sickle cell anemia . . . . .	99

3.6.1	Molecular dynamic simulation with NAMD	103
3.6.2	Conformational change analysis	106
3.6.3	PCA analysis	109
3.6.4	Correlation analysis with HbS interaction	110
3.7	Conclusion	112
	References	112

## **Chapter 4 Structural, Mechanical and Functional Properties of Intermediate Filaments from the Atomistic to the Cellular Scales** 117

4.1	Introduction	117
4.1.1	Hierarchical structure of vimentin intermediate filaments	121
4.1.2	The structural and physiological character of keratin	131
4.2	Connecting filaments to cells level function and pathology	135
4.2.1	Bending and stretching properties of IFs in cells	136
4.2.2	IFs responding differently to tensile and shear stresses	137
4.2.3	Mechanotransduction through the intermediate filament network	138
4.3	Experimental mechanics	138
4.3.1	Single filament mechanics	138
4.3.2	Rheology of IF networks <i>in vitro</i>	139
4.3.3	IF networks rheology in cells	140
4.4	Case studies	141
4.4.1	Single vimentin filament mechanics	141
4.4.2	Network mechanics	152
4.4.3	The mechanical role of intermediate filament in cellular system	156
4.5	Conclusion	158
	References	159

## **Chapter 5 Cytoskeletal Mechanics and Rheology** 167

5.1	Introduction	167
5.2	Modelling semiflexible filament dynamics	170
5.3	Experimental measurements	173
5.3.1	Glass microneedles	174
5.3.2	Cell poking	174

5.3.3	Atomic force microscopy ·····	175
5.3.4	Micropipette aspiration ·····	176
5.3.5	Microplates ·····	176
5.3.6	Parallel-plate flow chambers ·····	177
5.3.7	Optical tweezers ·····	177
5.3.8	Magnetic traps ·····	178
5.4	Computational models ·····	178
5.5	Conclusion ·····	183
	References ·····	183

## **Chapter 6 On the Application of Multiphasic Theories to the Problem of Cell-substrate Mechanical Interactions ·····**

6.1	Introduction ·····	190
6.2	The physics of contractile fibroblasts and their interactions with an elastic substrate ·····	192
6.2.1	Cell spreading, contractility and substrate elasticity ···	192
6.2.2	Molecular mechanisms of cell contractility ·····	194
6.3	Multiphasic mixture theory and cell contractility ·····	197
6.3.1	The cytoplasm as a quadriphasic medium ·····	198
6.3.2	Mass transport and mass exchange within the cell ···	201
6.3.3	Contractility and force balance ·····	205
6.3.4	Model's prediction for simple cases ·····	209
6.4	Interaction between contractile cells and compliant substrates ·····	212
6.4.1	Two-dimensional plane stress formulation ·····	212
6.4.2	Numerical strategy: XFEM-level methods ·····	213
6.4.3	Analysis of mechanical interactions between a contractile cell and an elastic substrate ·····	216
6.5	Summary and conclusion ·····	218
6.5.1	Summary ·····	218
6.5.2	Limitations of the multiphasic approach ·····	219
6.5.3	Concluding remark ·····	220
	References ·····	221

## **Chapter 7 Effect of Substrate Rigidity on the Growth of Nascent Adhesion Sites ·····**

7.1	Introduction ·····	225
7.2	Model ·····	227

# Chapter 1 Modeling and Simulations of the Dynamics of Growing Cell Clusters

Ignacio Romero\* and Juan J. Arribas

*Technical University of Madrid*

---

**Abstract:** A phenomenological discrete model for the dynamics of growing cell clusters is presented. Each cell is modeled as a growing deformable solid which can interact mechanically with its neighbors by means of adhesion and repulsion forces. By defining simple behavior rules based on the age and the mechanical state of the cells, simple cluster dynamics can be reproduced. The framework is far from complete, but describes the essential features required for more complete mechanical simulations of cell ensembles.

Keywords: cell mechanics, finite elements, population dynamics, cellular automata

---

## 1.1 Introduction

The study of cell cluster dynamics is fundamental for understanding biological phenomena such as embryology, tissue repair, and most importantly, solid tumors. Up to now, biochemistry has been the main discipline employed to study such processes, with undeniable success. There is, however, growing awareness that mechanics also plays a crucial role in these dynamical processes and new avenues to research and analysis are now opened.

Since the classical work of Young<sup>[1]</sup> and later Eaves<sup>[2]</sup>, the mechanical effects on tumors have been widely studied. For example, in the key work of Helmlinger et al.<sup>[3]</sup> experimental evidence was provided to support the idea that the growth of multicellular tumor spheroids is controlled by pressure. More surprisingly, their findings are demonstrated “... *regardless of host species, tissue of origin, or differentiation state.*” These, and similar ones<sup>[4,5]</sup> motivate the study of single cell mechanics, multiple cell mechanical interactions, and their effect on the global dynamics of growing ensembles.

Several approaches have been investigated to understand the mechanics of

---

\*Corresponding author, E-mail: ignacio.romero@upm.es.

growing cell clusters, cancer in particular<sup>[6]</sup>. The oldest models employ partial differential equations that treat tumors as continua with deterministic growth (see [7] and references therein). While these approaches allow of the study of complete tumors, they can not provide enough details of the mechanical effects at the micro scale, since cells are smeared out and are not represented.

The second type of approaches employed for studying cell population dynamics is based on cellular automata (see [8-10] among many others). These methods represent individual cells and their behavior, so they allow much richer resolution than smeared models. In an effort to keep the computational cost low, many of the geometrical/mechanical details are often ignored. Some cellular automata include sophisticated discrete evolution laws, and even some crude mechanical behavior.

The computational model that is presented in the current work advocates the use of individual entities to represent each cell in the cluster, just as cellular automata. However, in contrast with the latter, the proposed models have sufficient mechanical and geometrical details so as to replicate, at least qualitatively, the most important phenomena that seem to be at the heart of their mechanical behavior. The underlying motivation is to provide a test-bed for the mechanical response of cell clusters based on first principles and as few ad hoc evolution rules as possible. This environment will allow test hypothesis on the effect of mechanical variables on growth or elimination of cell colonies while providing very high definition pictures of the geometry and internal variables of the ensembles.

The basic mechanical features that are represented in the model are: deformation, material response, growth, adhesion, and repulsion. To replicate *in silico* all these effects, a nonlinear finite element model is employed. In it, every single cell is defined as a Deformable solid of ellipsoidal shape capable of following complex deformation modes. The material for each body is homogeneous and isotropic whose constants are chosen so as to qualitatively match experimental results. Growth, an attribute that most cellular automata do not incorporate, is described in a mechanically sound manner, whose rate is predetermined based on each cell's age. A key ingredient of the model is the numerical treatment of cell-to-cell interaction forces. The computational cost of a molecule-based, membrane-to-membrane interaction model is prohibitive. Thus, a macroscopic model is incorporated into the finite element computations using standard penalty constraints and surface-to-surface potentials. Finally, a decision tree is employed to capture the most basic events of the life cycle of each cell. At each instant, a cell might be divided or die depending on random decisions whose probability function depends on the cell's age and its mechanical stresses.

The model described in the current article still fails to become predictive.

In order to do so, larger number of cells need to be considered in each cluster, and additional effects should be incorporated into the model (among others, transport of nutrients and oxygen, pH, etc). Nevertheless, it provides a higher level of resolution than cellular automata and will be progressively improved and validated.

The outline of the rest of the article is as follows: In Section 1.2 the geometrical description of individual cells is discussed, both at the continuum and the computational levels. Then, in Section 1.3, their mechanical equilibrium is formulated. Section 1.4 describes the two mechanical interactions which are considered among cells, namely, interpenetration constraints and adhesion. The simplified logic for the life cycle of each cell is presented in Section 1.5 and details of the whole numerical implementation are provided in Section 1.6. A large-scale numerical simulation of hundreds of interacting cells is described in Section 1.7, using all the model features presented before. The article concludes with a summary of results in Section 1.8.

## 1.2 Single cell geometry and kinematics

In order to model the salient features of deformable growing cells, a deformable body is defined whose mechanical response resembles that of a cell. Sophisticated cell mechanical models can be found in the literature that are used to study various aspects of the cell deformation. They employ either tensegrities to reproduce the mechanical response of the cytoskeleton as in, for example, [11, 12], or continuum finite elements as in [13, 14]. In all cases, high accuracy in reproducing simple mechanical tests can only be obtained at the expense of complex equations and computational models, which, in practice, preclude their use for studying the joint behavior and interactions of hundreds of cells. In this work, rather than attempting to accurately model the mechanics of individual cells, we identify the *essential* mechanical features of their behavior and model them, at least, in a qualitatively correct fashion.

We propose next an isotropic, homogenized cell model that accounts, in an approximate manner, for the mechanical response of the cell, its membrane, its cytoskeleton, organelles, etc. The equations are the standard equilibrium partial differential equations of a deformable nonlinear solid with growth. In this section we focus on their geometric description and kinematics, including growth. Both the continuum and numerical models will be described, illustrating the generality and flexibility of the approach.

### 1.2.1 The continuum model

Each cell is assumed to be a set of particles that occupy, in the reference growth-free configuration, an open set  $\mathcal{B}_o$  of  $\mathbb{R}^3$  and particles labeled by  $\mathbf{X}$ . At time  $t$ , the cell occupies a region  $\mathcal{B}_t \in \mathbb{R}^3$ . Particles  $\mathbf{X} \in \mathcal{B}_o$  are mapped onto points  $\mathbf{x} \in \mathcal{B}_t$  by the deformation  $\varphi$  so that  $\mathbf{x} = \varphi(\mathbf{X}, t)$ .

The deformation gradient  $\mathbf{F}_t = \mathbf{grad}[\varphi]$  is the function that maps neighborhoods of  $\mathbf{X}$  onto their deformed counterpart at  $\mathbf{x}$ . By assumption, we consider motions so that the deformation gradient is of the form

$$\mathbf{F} = \mathbf{F}_d \mathbf{F}_g. \quad (1.1)$$

The term  $\mathbf{F}_g$  accounts for the growth of the material and it is assumed, in our model, to be known a priori. The term  $\mathbf{F}_d$  is the part of the deformation gradient that is associated with strains and stresses, and the only part that enters the formulation of the material model. Hence, we define the right Cauchy–Green deformation tensor as

$$\mathbf{C} = \mathbf{F}_d^T \mathbf{F}_d. \quad (1.2)$$

See Fig.1.1 for an illustration of this kinematic concept.

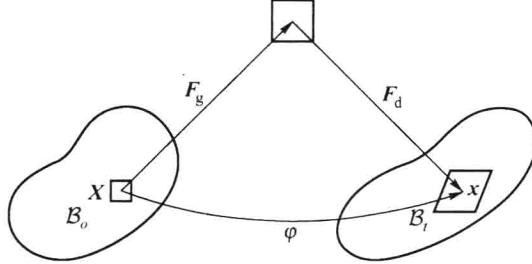


**Fig. 1.1** Cell kinematics, including growth, described at the differential level.

In living organisms, growth is controlled by space, nutrients, biological signals, etc, and it is anisotropic in general. In the proposed framework, however, we will employ the simplest model of growth that will allow us to concentrate on the mechanical phenomena. It consists of an *ad hoc* rule for the growth part of the deformation gradient which, furthermore, is homogeneous, isotropic and of the form

$$\mathbf{F}_g(\mathbf{X}, t) = g(t) \mathbf{I}. \quad (1.3)$$

In the previous equation  $g : [0, \infty) \rightarrow [1, G]$  is a continuous, monotonically increasing function from 1, the reference un-grown state, to  $G$ , a constant related to the volume of the adult cell.

### 1.2.2 The numerical model for the cell geometry

Every cell is discretized with a nonlinear finite element model. A special mesh generator has been defined to create cells of ellipsoidal shape with arbitrary dimensions and with selectable mesh density. Other types of cell geometry could be used, since this step is completely independent of the rest of the model but, for simplicity, results shown in this article are restricted to random ellipsoidal geometry (or spherical, as a special case).

Figure 1.2 shows three identical cells with three different mesh densities. For the dynamic simulations it is crucial that cells can be created/eliminated automatically, and that the end user only selects the desired resolution. This choice has the most dramatic impact on the overall CPU cost of all other assumptions.

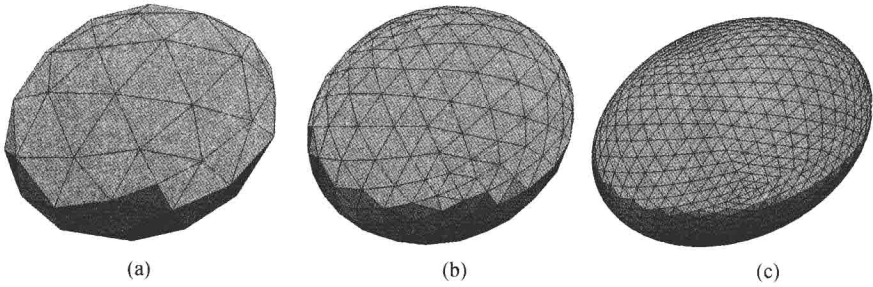


**Fig. 1.2** Three cell meshes with different levels of mesh refinement.

## 1.3 Single cell equilibrium and material model

The equilibrium equations of mechanics are imposed over every volume element of the cell using a nonlinear finite element formulation. This solution step is exact, up to the finite element error, and accounts for every internal stress and strain component in the cell.

### 1.3.1 Cell equilibrium

The equilibrium equations of the cell are the standard balance of equations in continuum mechanics. If  $\mathbf{S}$  is the second Piola–Kirchhoff stress tensor, then the balance of linear momentum can be stated as

$$\begin{aligned} \operatorname{div} [\mathbf{F}\mathbf{S}] &= \mathbf{0} & \text{in } \mathcal{B}_g, \\ \mathbf{F}\mathbf{S}\mathbf{N} &= \mathbf{T} & \text{on } \partial\mathcal{B}_g. \end{aligned} \quad (1.4)$$

In the previous equations, operator  $\text{div}[\cdot]$  is the material divergence and  $\mathbf{T}$  is known forces on the cell boundary. Alternatively, the equilibrium can be formulated as the position that minimizes the potential energy

$$V(\boldsymbol{\varphi}) = \int_{B_o} W(\mathbf{grad}[\boldsymbol{\varphi}], \mathbf{F}_g) dV + V_{\text{ext}}(\boldsymbol{\varphi}) , \quad (1.5)$$

where  $W$  is a stored energy function on the cell material and  $V_{\text{ext}}$  is the potential of the external forces.

In an abstract way, the solution of the mechanical cell problem consists in finding  $\boldsymbol{\varphi}$  given a known growth law  $\mathbf{F}_g$  and known surface tractions  $\mathbf{T}$ . Details of the formulation and solution of Eq.(1.4) in the context of the finite element method can be found in standard references. See, for example, Ref. [15].

To close the formulation of the boundary value problem of single cell mechanics suffices to define a constitutive law for the homogenized material.

### 1.3.2 The material model

The choice of constitutive law is completely independent of the rest of ingredients of our model. Hence, any sensible model could be employed, possibly incorporating finite strain elastic, viscous, or even plastic effects.

In our simulations we have employed hyperelastic material models, the simplest ones that might be used to approximate the most elementary mechanical behavior as reported throughout the literature regarding “traction” tests of the cells<sup>[16,17]</sup>. The goal is to obtain cell-like deformable solids whose mechanical response resembles that of typical cells. To this end, a standard neo-Hookean model is employed as defined in [18]. The symmetric Piola-Kirchhoff stress tensor is thus defined by  $\mathbf{S} = 2\partial_{\mathbf{C}}W$ , where  $W$  is the stored energy function of the form

$$W = U(J) + \frac{\mu}{2}(I_1 - 3) - \mu \log J, \quad U(J) = \frac{\lambda}{2}(\log J)^2 , \quad (1.6)$$

with  $I_1 = \text{tr}[\mathbf{C}]$  and  $J = \sqrt{\det(\mathbf{C})}$ . The two elastic constants  $\lambda, \mu$  are obtained by fitting experimental data with the model.

### 1.3.3 Determination of material constants

In order to select representative elastic constants for Eq.(1.6) we use the experimental data provided in [19]. In this reference force-displacement curves are reported for compression tests performed over C2C12 mouse myoblasts.

It is not the goal of this modeling phase to find the value of the elastic constants of the material that these cells are made of. Rather, a phenomenological value is sought out so that when a cell of the type described in Section 1.2 is employed in a numerical simulation, its overall response matches the experimental results. This distinction is relevant because it allows us to employ relatively coarse finite element meshes without unacceptable levels of inaccuracy, at least in the dominant deformation modes. In turn, this results in material constants which are mesh-dependent. In the simplest possible model in this section, a single node is defined in the cell interior. This crude discretization is sufficient for a qualitative approximation.

In our simulations a spherical cell-like body of volume  $2\,520\,\mu\text{m}^3$  is considered. The material model is neo-Hookean with stored energy function defined in Eq.(1.6). For each level of mesh refinement, the corresponding Young's moduli and Poisson's ratio are obtained to fit the experimental data of the compression tests. For the coarse mesh, the one employed in the rest of the simulations, the elastic constants found have values  $\lambda = 40.3\,\text{kPa}$  and  $\mu = 4.48\,\text{kPa}$ .

To carry out the simulation, a fully grown cell is placed between two rigid surfaces which are brought close to each other, compressing the cell and deforming it. Figure 1.3 shows four stages during the compression test and Fig.1.4 depicts the compression force vs. the relative diameter change obtained with the numerical model described above, superimposed to the experimental results alluded to above. The agreement is good enough for qualitative purposes. The change of slope in the deformation curve is due to the discretization error in the coarse mesh employed.

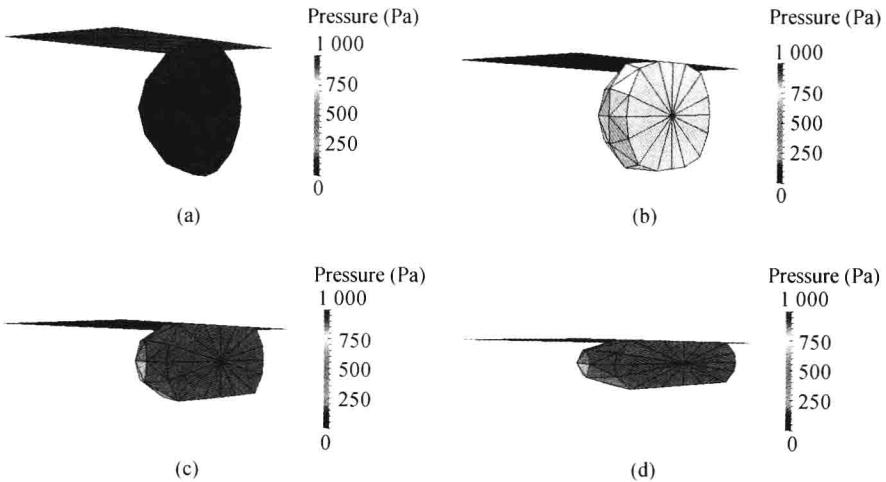


**Fig. 1.3** Cell compression test. The cell is cut through a vertical plane to show the stress distribution in the inside (color plot in the book end).

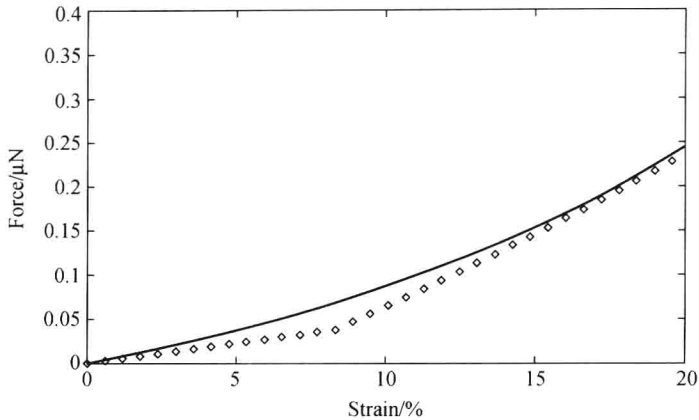


**Fig. 1.4** Compression force vs. relative diameter change in the compression test of a cell-like spheroid. The continuous line shows a fit of the experimental results reported in [19]. The dots correspond to the numerical results obtained with the numerical model.

## 1.4 Modeling cell interactions

Having defined a model for individual cells, it remains to incorporate the rules that will serve to represent the interaction between cells, eventually governing the global system dynamics. As in the case of single cells, it is not trivial to determine which complex interactions should be considered, and which should be neglected. In any case, and as before, it is not possible to attempt modeling all interactions. Rather, one should aim to select the ones that most crucially affect the overall response.

The most fundamental effect of mechanical nature among cells is attraction/repulsion forces. The detailed picture of cell-to-cell forces is described in detail in the literature [20] and their accurate description might be crucial for the study of certain problems<sup>[21]</sup>. In our analysis, having already made simplifications at the level of the cell mechanics, it becomes reasonable to attempt again to capture the most basic effects in a qualitatively correct way, but without excessive complexity that would preclude a full numerical solution.

With these considerations we aim to model cell repulsion first. The micromechanical mechanisms behind cell interpenetration are complex and would require a high resolution of the cell geometry<sup>[22,23]</sup>. Using, for example, Lennard–Jones type potentials to model such effect would entail almost a molecular description of the cell membrane. Instead, we propose to coarse grain all the repulsive forces within the variational formulation of the prob-

lem (as required for the finite element implementation) using the simplest penalty method. Using this standard technique<sup>[24]</sup>, the penetration of the two external surfaces of the cell is “artificially” avoided. Of course, the repulsion forces no longer are physically based, but they nevertheless account for the right amount of resultant guaranteeing the constraint.

Cell adhesion is also represented in the model. As before, the micromechanical causes for such forces are complex and their detailed resolution is outside the goals of the current model. We propose to model them by defining a surface-to-surface attraction that accounts for these effects. As described below, it can be easily incorporated within the finite element formulation and adjusted so as to fit experimental data.

### 1.4.1 Cell-to-cell contact

Interpenetration forces guarantee that two cells, even when they get close to or pressed against each other, do not overlap. Ignoring their molecular explanation, their overall effect can be described in a purely geometrical manner and, in this sense, easily implemented. In fact, at the cell scale, these forces can be described as contact forces. This type of interactions has been thoroughly studied in the context of Solid Mechanics and its numerical implementation is well documented<sup>[25,26]</sup>.

The simplest numerical strategy to enforce interpenetration is based on penalization. Given two cells  $\mathcal{B}_1, \mathcal{B}_2$ , let  $\Gamma_1, \Gamma_2$  denote, respectively, their boundaries. For each point  $\mathbf{X}_1 \in \Gamma_1$ , the signed distance to  $\Gamma_2$  is denoted  $\Delta(\mathbf{X}_1)$ , and defined as being positive if  $\mathbf{X}_1$  is outside  $\mathcal{B}_2$  and negative otherwise. Then, the penetration of  $\mathbf{X}_1$  is defined as

$$\pi(\mathbf{X}_1) = \langle -\Delta(\mathbf{X}_1) \rangle, \quad (1.7)$$

where  $\langle \cdot \rangle$  denotes the Macaulay bracket. By symmetry, the same argument applies to the penetration of the  $\mathcal{B}_2$  into  $\mathcal{B}_1$ . Then, to enforce the interpenetrability of either body into its neighbour it suffices to augment Eq.(1.5) by the penalization term

$$\int_{\Gamma_1} \frac{\kappa_p}{2} \pi(\mathbf{X})^2 \, dS + \int_{\Gamma_2} \frac{\kappa_p}{2} \pi(\mathbf{X})^2 \, dS. \quad (1.8)$$

The penalization constant  $\kappa_p$  must be positive and large in comparison with any characteristic stiffness of the cell. Recommendations for the choice of this contact constants are provided in standard texts on finite elements and we refer to the references alluded to before.

### 1.4.2 Cell-to-cell adhesion

When the surfaces of two neighboring cells become close, adhesion forces appear that try to bring them together and to keep them in this way. As in the case of the repulsion forces, we propose a phenomenological model that accounts for this type of interactions in such a way that it is qualitatively correct and matches closely experimental data. Following the results reported in [19], adhesion forces are incorporated between membrane surfaces closer than a cut-off distance  $\delta_o$ . Based on the experimental data of this article, adhesion forces per unit of surface on one cell and unit of surface of the opposing cell have constant value  $\kappa_a$  as long as their relative distances are below  $\delta_o$ , and zero otherwise.

Let  $\gamma_1 = \varphi(\Gamma_1)$  and  $\gamma_2 = \varphi(\Gamma_2)$  be the boundaries of the deformed cells. To include adhesion effects on the formulation, an additional force per unit area of the surface  $\gamma_1$  must be added at each point  $\mathbf{x}_1 \in \gamma_1$  of the form

$$\mathbf{F}_1(\mathbf{x}_1) = \int_{\gamma_2} \mathbf{f}(\mathbf{x}_1, \mathbf{x}_2) \, dS_2, \quad (1.9)$$

where the force  $\mathbf{f}$  per unit of area squared has value

$$\mathbf{f}(\mathbf{x}_1, \mathbf{x}_2) = \kappa_a \mathcal{H}(\delta_o - |\mathbf{x}_2 - \mathbf{x}_1|) \frac{\mathbf{x}_2 - \mathbf{x}_1}{|\mathbf{x}_2 - \mathbf{x}_1|}, \quad (1.10)$$

and  $\mathcal{H} : \mathbb{R} \rightarrow \{0, 1\}$  is the Heaviside step function. Similarly, points on the surface  $\gamma_2$  are attracted to  $\gamma_1$  with a force per unit area

$$\mathbf{F}_2(\mathbf{x}_2) = \int_{\gamma_1} \mathbf{f}(\mathbf{x}_2, \mathbf{x}_1) \, dS_1. \quad (1.11)$$

From the previous two equations it follows that

$$\int_{\gamma_1} \mathbf{F}_1(\mathbf{x}_1) \, dS_1 + \int_{\gamma_2} \mathbf{F}_2(\mathbf{x}_2) \, dS_2 = \mathbf{0}. \quad (1.12)$$

The Equation (1.10) models adhesion forces of constant moduli (per unit of surface squared) when the distance between the interacting surfaces is below a threshold  $\delta_o$ . This represents bonds that are created when the cell membranes are close to each other and only break when separated beyond  $\delta_o$ .

To implement the adhesion force on the surface  $\gamma_1$  (respectively  $\gamma_2$ ) the following integral must be evaluated

$$\int_{\gamma_1} \mathbf{F}_1 \, dS_1 = \int_{\gamma_1} \int_{\gamma_2} \mathbf{f}(\mathbf{x}_1, \mathbf{x}_2) \, dS_2 \, dS_1. \quad (1.13)$$

In the context of a finite element model, the previous integral is approximated with the finite sum

$$\int_{\gamma_1} \int_{\gamma_2} \mathbf{f}(\mathbf{x}_1, \mathbf{x}_2) dS_2 dS_1 \approx \sum_{T_i \in \gamma_1} \sum_{T_j \in \gamma_2} \mathbf{f}(C_i, C_j) A_i A_j, \quad (1.14)$$

where  $T_i, T_j$  are the triangles on the cell surfaces,  $C_i, C_j$  their centers, and  $A_i, A_j$  their corresponding areas.

### 1.4.3 Cell-to-cell interaction test

To illustrate the effect of the two types of cell interactions defined in this section we show next some results of the virtual test of two cells interacting coming into contact with each other, and then pulled apart.

Two identical spherical cells of initial diameter  $5.6 \mu\text{m}$  are placed with their centers fixed at a distance also of  $5.6 \mu\text{m}$ . Growth in the cells progressively increases their volume, eventually multiplying its original value by 3. Then, due to their proximity and the restriction on their centers, both cells come into contact, deforming while they press one against the other.

Once the two cells are fully grown and the contact forces are developed, they are slowly pulled apart. In this process, the contact forces are reduced. Eventually, the two previously contacting surfaces no longer try to interpenetrate and adhesion forces are then activated which attempt to keep them together.

Figure 1.5 describes a complete sequence of the contact/adhesion test. Pressure builds up when the two cells are pressed one another, especially close to the interacting surfaces. When the two bodies are separated, pressure decreases and adhesion pulls the two cells together. Figure 1.6 plots the values

